JOURNAL OF MATERIALS SCIENCE 29 (1994) 4184–4190

Direct observation of the fracture of CAS-glass/SiC composites

PART II *Notched tension*

H. R. SHERCLIFF, P. W. R. BEAUMONT
Engineering Department, Cambridge University, Trumpington St, Cambridge, CB2 1PZ, UK
G. VEKINIS
"Demokritos" National Centre for Scientific Research, Institute of Materials Science, 15310 Ag. Paraskevi Attikis, PO Box 60228, Athens, Greece

The fracture behaviour of a CAS-glass/SiC-fibre-reinforced composite was observed by dynamic *in situ* scanning electron microscopy (SEM). In a companion paper [1], tests on common delamination geometries are described and the basis of micromechanics models is critically evaluated. Flexure geometries and also the unnotched tensile response of ceramic-matrix composites (CMCs) have received considerable attention, both theoretically and experimentally. The effect of through-thickness notches on the tensile fracture of CMCs has however been relatively neglected. Previous work on polymer-matrix composites demonstrates the strong influence of subcritical damage on the fracture behaviour. In this paper we examine failure of notched CAS-glass/SiC composites in tension, under static- and fatigue-loading conditions, using a combination of *in situ* and conventional test methods. The subcritical damage which forms is compared with that in polymer-matrix composites, and the consequences for prediction of the notched strength are discussed.

1. Introduction

The tensile response of ceramic-matrix composite (CMC) laminates with through-thickness notches is important from the design point of view. Mechanical joining of CMC components or holes to permit gas flows necessitates the use of holes through the laminate. Many studies on CMCs have concentrated on their unnotched behaviour, notably on the problem of matrix cracking and the associated mechanics of fibre bridging [2–8]. Fracture-mechanics methods have been developed extensively to describe bridged mode-I cracks, including those which propagate from notches [9–14]. These models have shown that failure by propagation of a bridged mode-I crack is strongly specimen dependent, that is, controlled not only by the mode of loading but also by the relative sizes of the specimen notch, width and crack length.

While mode-I cracks have been observed to propagate from notches [10], mixed-mode cracking frequently occurs as the weak fibre–matrix interface leads to low resistance to shear loading parallel to the fibres. Tensile loading (either uniaxial or flexure) of notched material then leads to the formation of splits and delaminations parallel to the fibres and tensile axis. This damage can alter the stress state at the notch root considerably, and thereby lead to completely different failure criteria. This problem has been addressed in polymeric composites in a series of studies at the Cambridge University Engineering Department [15–24]. The aim of the present study is to evaluate the tensile fracture of a CMC in the light of this work.

The damage mechanics of notched carbon-fibre–epoxy (CFRP) laminates was observed *in situ* and modelled by Kortschot and Beaumont and others [15–18]. The damage evolution from double-edge-notched specimens loaded in tension was found to grow in a self-similar manner in a range of layups, and was characterized by: (a) splits from the notch root parallel to the fibres in the 0° plies; (b) narrow 0/90 delaminations associated with each split; and (c) transverse ply cracks, concentrated around the delamination zones. A predictive model for the notched strength was produced, incorporating the observed damage into a finite-element model of the specimen.

Spearing *et al.* [19–22] subsequently extended the models to fatigue loading, with centre-notched specimens, and they included the loss of stiffness caused by damage growth. The first step in all this work has always been to obtain a clear picture of subcritical cracking and the *terminal damage state* at failure, before embarking on numerical modelling of the stress state in the material, since this depends critically on the damage. Fig. 1 shows an X-ray micrograph of the damage which is typically observed in a CFRP, in this case from a centre notch. In a CFRP the damage shows reasonable symmetry between the four splits in a given 0° ply, growing with increasing stress in a self-similar manner, until the 0° plies fail at the notch root.

0022–2461

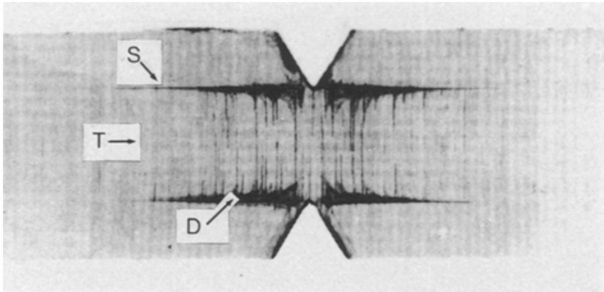

Figure 1 A typical X-ray image of a (90/0)s CFRP centre-notched specimen showing the damage which develops: (S) splits, (D) delaminations, and (T) transverse ply cracks. Contrast is achieved by infiltrating the crack with ZnI_2 penetrant (taken from [25]).

In fatigue, the damage continues to propagate to greater split lengths than are obtained in static loading. The effect of the longer splits and delaminations is to reduce the stress concentration and thereby raise the failure strength above the quasistatic value, while leading to a loss of stiffness due to the higher crack density. The criterion for failure of the main load bearing 0° plies took due account of the statistical (Weibull) variation of the strength of the material. It is implicit in the model that the intrinsic strength of the 0° plies is not degraded by fatigue loading (for example, by fibre failure).

The work of Kortschot and Spearing has illustrated the notch insensitivity of CFRPs by evaluating the reduction in the stress concentration at the root of a notch caused by the propagation of subcritical damage. Further studies have tested the generality of the concepts in other polymer-matrix systems (for example, carbon–PEEK (poly-ether-etherketone) [23]; glass–epoxy and Kevlar–epoxy [24]). The question therefore arises as to whether similar behaviour is found in CMC systems, and whether similar models for tensile failure can be proposed. Some initial studies of carbon-matrix SiC- and C-fibre composites have recently been reported [26, 27], but this area has clearly received less attention experimentally than unnotched tension and flexure testing. A range of tests was therefore conducted on double-edge-notched specimens of CAS-glass/SiC laminates (CAS is defined in Section 2.1), to examine the development of subcritical damage and the final failure. This test series was conducted partly using conventional testing machines due to the use of both static and fatigue loading, and limitations of load levels on the *in situ* facility. The tests were interrupted for SEM examination to maintain a consistent standard of observation of the behaviour with the dynamic *in situ* tests.

2. Experimental work, results and discussion

2.1. Material

The laminated material supplied by the USAF Materials Laboratory, Dayton, consisted of various layups of CAS (calcium–alumino–silicate) glass reinforced by Nicalon SiC fibres. This material is described in Part I [1]. Double-edge-notched tension specimens were machined from a plate of a $(0/90/0)_S$ laminate using diamond cutting tools. The specimen widths were between 4 and 6 mm, and notches were cut in one of three shapes: V-notch, rectangular or semicircular.

2.2. Static tests – double-edge-notched tension

2.2.1. *In situ observations of damage and failure*

The first test was conducted *in situ* using a V-notch (see Fig. 2). The ratio of the total notch depth, $2a$, to the specimen width, w, was approximately 0.7 in this test, but this decreased to 0.5 for all subsequent tests. The first cracks observed were transverse ply cracks (TPCs) in the notch root, followed by delaminations along the 0/90 interfaces which grew with increasing load. The delaminations were not clean interface cracks but tended to deviate into the 90° plies and become TPCs. Fig. 3a shows a view into the notch shortly before specimen failure – the damage is somewhat asymmetrical with longer delaminations to the right of the notch. Cracks also formed in the 0° ply at the notch root (Fig. 3b). By analogy with polymeric systems, it was assumed that these were splits parallel to the fibres, and this was verified when the surface of the laminate was also observed in subsequent tests.

When the damage state was as shown in Fig. 3a, catastrophic failure occurred; see Fig. 4a. The TPCs which opened up at failure were not at the notch root, and many of the 0° fibres also failed away from the root, leading to extensive pull-out (Fig. 4b). Examination of the fracture surfaces revealed pull-out of single fibres and also fibre bundles (Fig. 5).

To sum up the observations of this static tensile test: (a) delaminations and TPCs form, accompanied by splits in the 0° plies; (b) the damage can be somewhat asymmetrical; (c) at a particular damage state, catastrophic failure occurs; and (d) fibre failure is not concentrated at the root of the notch, but is diffused through a considerable volume of material to either side, leading to extensive fibre pull-out.

The type of damage which forms is therefore broadly similar to that observed in polymeric systems. The TPC density is much lower than in CFRP, and the material also appears to delaminate more easily, since the delaminations grew further up the notch flanks than would be observed in CFRP. The failure process differs more markedly: carbon-fibre–epoxy laminates always fail at the notch root, but failure of the CAS-glass/SiC material is not so localized, in spite of the stress concentration of the notch. The statistical variability of the fibre and ply strength is thus more

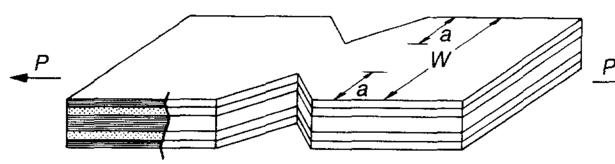

Figure 2 A schematic of a double edge-notched (DEN) tensile specimen.

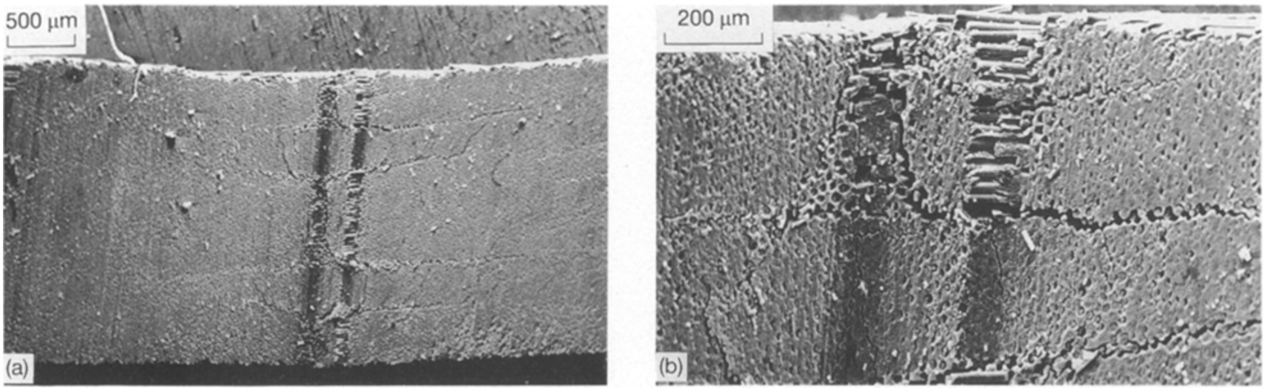

Figure 3 Damage in a DEN test on a CAS-glass/SiC $(0/90/0)_S$: (a) formation of delaminations and transverse ply cracks; and (b) delaminations, splits and TPCs in the top 0/90 plies at a higher load.

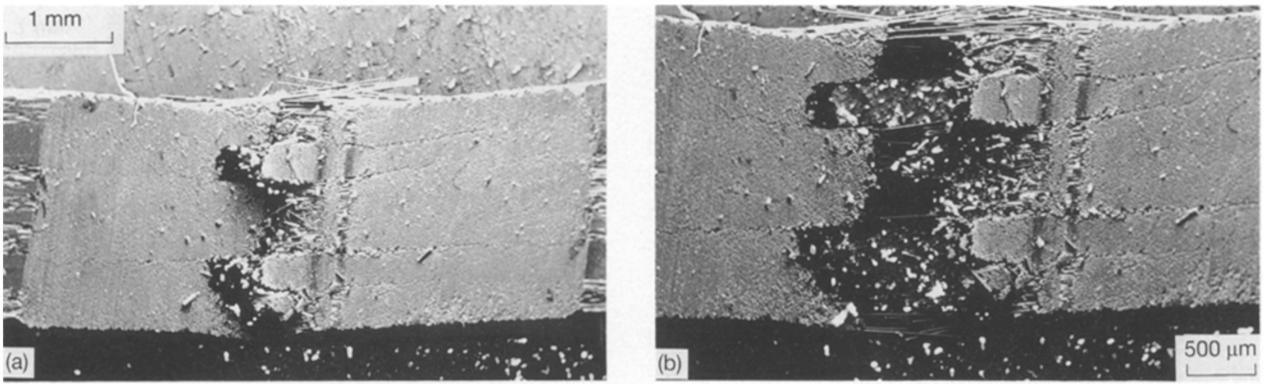

Figure 4 SEM micrographs of failure in a DEN test: (a) a view of the whole notch region immediately after failure, (b) a view of the whole notch region after extensive pull-out, with some 0° fibres still bridging the fracture.

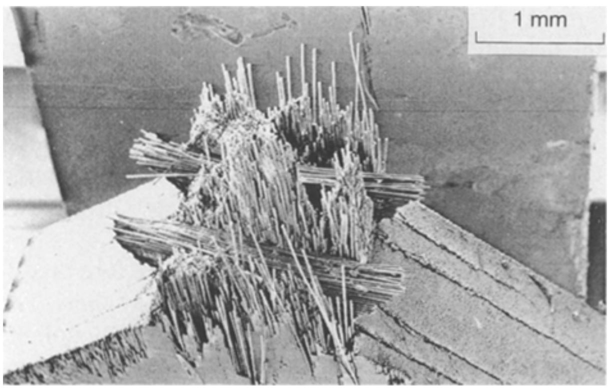

Figure 5 SEM micrographs of the two fracture surfaces, showing extensive fibre pull-out, and 90° ply failure away from the notch root.

significant, so fibres fail in a greater volume of material. This has also been noted as a deviation in the behaviour of glass–fibre epoxy laminates from that of CFRPs [24]. The CAS-glass/SiC material is therefore relatively notch insensitive.

The *in situ* test with a V-notch thus indicated some parallels and some differences between the CAS-glass/SiC material and conventional polymeric composites. There were, however, some drawbacks with this test: (i) the loads required were around 2 kN, which approached the limit of the *in situ* rigs; (ii) only damage in the notch could be observed, whereas it was desirable to see both the notch and specimen surface simultaneously; and (iii) the roughness of the notch flanks did not allow a very clear view of damage accumulation. Furthermore, fatigue loading *in situ* could only be realistically achieved over 10 or 20 cycles. Subsequent tests were therefore conducted on conventional screw-driven test machines, but were interrupted for SEM observation of the damage using a rotating stage, which allowed all sides of the specimen to be observed. Alternative notch shapes were also used; these shapes were easier to prepare and gave a clearer view of the damage. This also allowed an evaluation of the influence of the notch shape on the failure process. For a more direct comparison with the CFRP work, the notch depth was also reduced to $2a/w = 0.5$.

2.2.2. The effect of the notch shape

2.2.2.1. Rectangular notch. Rectangular notches were cut using a 0.4 mm diamond wheel normal to the specimen edge. The root of the notch was flat with a good finish, so the initiation of cracks could be observed. The damage which formed followed the same pattern as in the V-notched test – Table I shows the remote stress applied at various levels of damage. The first damage was in the form of TPCs which formed at

TABLE I. Damage evolution with remote stress in double-edge-notched tension tests

Damage state	Remote stress (MPa)	Failure stress (%)
90 ° ply cracks at notch corners	87	46
90 ° ply cracks at notch centre and 0 ° ply matrix cracks	148	78
Delaminations and splits at some interfaces	169	89
Catastrophic failure	190	100

the sharp corners of the rectangular notch. Cracks at the notch centre formed at a higher stress. The remote stress for first cracking was surprisingly high, as the actual stress on the central ligament is at least twice the remote value. Multiple matrix cracks formed in the notch root in the 0 ° ply, some by extension of 90 ° cracks which had appeared at a lower stress (Fig. 6). Zawada *et al.* [28] also observed that 90 ° ply cracks precede 0 ° cracks in tests on the same cross-ply material with unnotched specimens; Pryce and Smith [29] and Beyerle *et al.* [30] have likewise observed 90 ° cracks extending into the adjacent 0 ° plies in CAS-ceramic/SiC materials. 0 ° ply cracks are important as they locally raise the fibre stress and thus influence the statistical failure of fibres.

Prior to failure, it was possible to see the splits in the surface 0 ° plies with the naked eye. Subsequent examination of the failed specimen (Fig. 7) clearly showed one surface split extending from the notch root. The splits were not single well-defined cracks but a narrow band of damage, several fibres in width. Note also that splits do not form at every possible location, but only in some of the 0 ° plies at the notch root. This again contrasts with CFRPs where splits form in all 0 ° plies with a considerable degree of symmetry. The smaller notch depth meant that the delaminations reached the specimen edge prior to failure, and propagated a considerable distance along the edge. In CFRPs the delaminations do not approach the free edge, so there is a greater tendency to delaminate in this material, even though the elastic anisotropy between 0 ° and 90 ° plies is very much smaller. Failure was accompanied by further propagation of both splits and

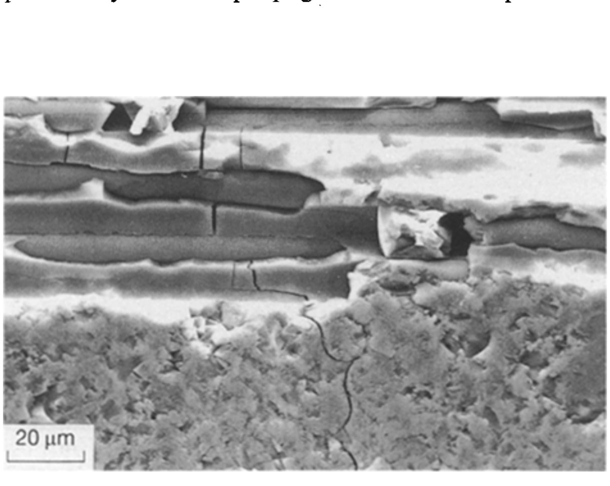

Figure 6 SEM micrographs of matrix cracks in the notch root – the 90° ply crack formed first and it later extended into the 0° ply.

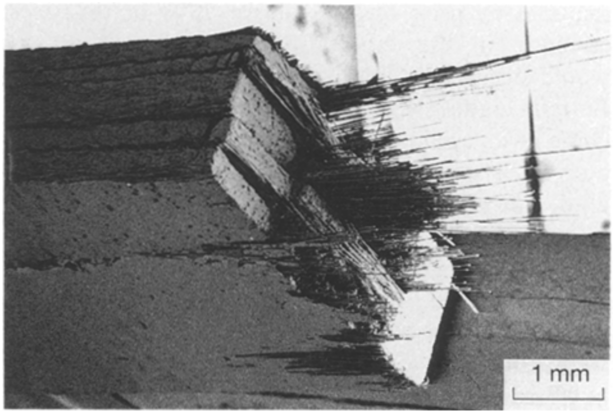

Figure 7 SEM micrographs of the fracture surface of a rectangular DEN specimen showing a surface split from the notch root.

delaminations, often right into the grips. The remote failure stress in two nominally identical tests was 231 and 190 MPa, which indicates considerable scatter in the extent of the damage which forms and in the local material strength.

2.2.2.2. Semicircular notch. Semicircular edge-notches were produced by drilling several holes in a plate with diamond drill bits 4 mm in diameter and then cutting out specimens through the hole centres. It was difficult to drill through the material without the 0 ° ply on the back face becoming damaged around the hole, even with a hard backing material. The static behaviour of a specimen with a semicircular edge notch, with $2a/w = 0.5$, was very similar to that with a rectangular notch, described above. Splits formed at around 80% of the failure load, and they were visible to the naked eye. The delaminations again extended from the notch root out to and along the free edge, so this was not an effect caused by a particular notch shape. The remote stress at failure was 211 MPa, which is halfway between the two values measured for rectangular-notched specimens. It therefore appears that for a given value of $2a/w$ the notch shape has little effect on the damage and failure stress – the stress concentration at the notch root is blunted by the splits and delaminations, which leads to significant notch insensitivity. The proximity of the notch root to the specimen edge is clearly important, as the stress concentration will change if the delaminations do not reach a free edge. Shortage of material did not allow further investigation of this effect.

2.3. Fatigue tests – double-edge-notched tension

2.3.1. Observations of damage and failure

Fatigue loading of CFRPs, causes static damage to propagate at a rate which falls steadily as the split length increases. Typically, maximum stresses of the order of 70% of the static failure stress are required in fatigue (for a minimum stress near zero) to cause measurable damage growth in under 10^6 cycles. Fatigue tests were therefore made on the CAS-glass/SiC material at peak stresses above 70% of the static strength, in the expectation that damage growth would occur in a relatively small number of cycles. Fatigue loading was achieved on a screw-driven machine in its cyclic mode, at a frequency of approximately 0.2 Hz. The R-ratio (minimum load/maximum load) was maintained at 0.1 throughout.

2.3.1.1. Semicircular notch. A specimen with a semicircular notch, $2a/w = 0.5$, was fatigued at $\Delta\sigma = 160$ MPa (for which σ_{max} was roughly 82 % of the static failure value). The first cycle was thus sufficient to initiate TPCs, splits and delaminations, close to the terminal static-damage state. After 150 cycles the damage had propagated, as illustrated in Fig. 8. Fig. 8a shows one face of the specimen – splits have grown from the notch roots in all four possible locations, but as bands of damage which have broadened towards the specimen centre near the lower notch. Viewed from the side (Fig. 8b) the damage in the 0° surface plies is clear, with many broken fibres protruding from the surface. Delaminations have also run along all the 0/90 interfaces down the specimen edge. Fig. 8c shows that the delaminations propagate one or two fibres away from the interface, but can run in both 0° or 90° plies (those in the lower 90° ply eventually linking up). The number of cycles was increased to 400, causing further damage propagation. Fig. 8d shows the same face as in Fig. 8a at $N = 400$; the 0° ply damage is more marked, additional splits having formed away from the notch root.

The specimen was then pulled to failure, which caused further damage; Fig. 9a shows the same face of the specimen after failure: the fibres have parted in a broad band between the notches, but the damage is extensive away from the notches too. On the opposite face however, the 0° ply failure is 5 mm to one side of the notch, linking the two splits (Fig. 9b). Long delaminations have formed, and they have opened up much more than in a static test. The residual strength after 400 cycles was 229 MPa, which is slightly higher than in the static test with this shape of notch, but it is essentially unchanged within the scatter of the data.

It is therefore clear that, in common with CFRP and other polymeric systems, fatigue loading causes damage propagation. In CFRP this reduces the stress concentration at the notch and increases the residual strength. This only occurs because the fatigue loading does not significantly influence the static strength of the 0° plies. It is apparent in CAS-glass/SiC however that the 0° plies are damaged by fatigue, with premature fibre failures occurring, so the strength would be reduced. Hence, for the conditions chosen here, the benefit of a reduction in the stress concentration has been cancelled out by a reduction in the ply strength. It is anticipated that further fatigue loading would eventually cause failure, as fibre failures will progressively raise the stress on the fibres remaining intact. However it is perhaps surprising that the strength of the material in the condition illustrated in Fig. 8d is still as high as in the unfatigued condition, though it is likely that there will have been some loss of stiffness.

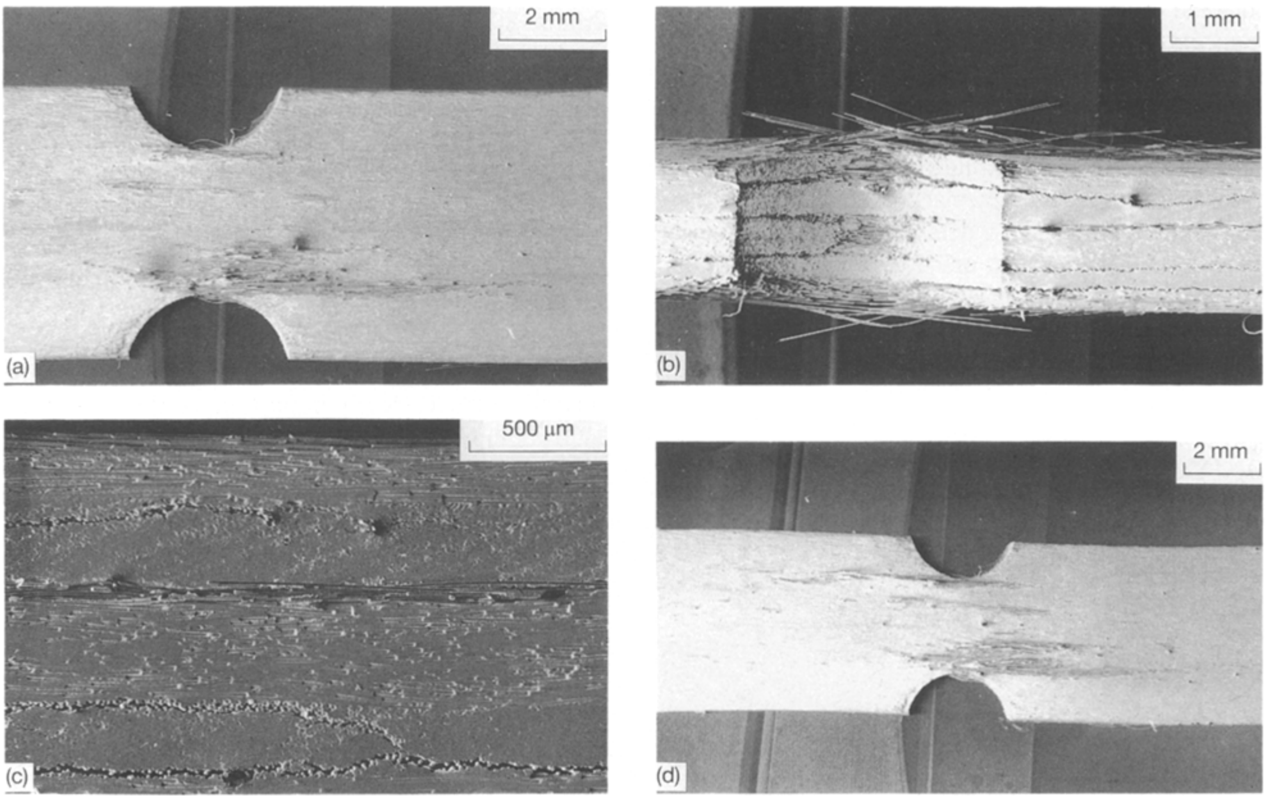

Figure 8 SEM micrographs of damage growth in fatigue loading of a semicircular DEN specimen, $\Delta\sigma = 160$ MPa, $R = 0.1$: (a) the surface of the specimen, after 150 cycles, (b) an edge of the view of the notch region, after 150 cycles, (c) two types of delamination crack along the specimen edge, (d) the surface (as in Fig. 8a) after 400 cycles.

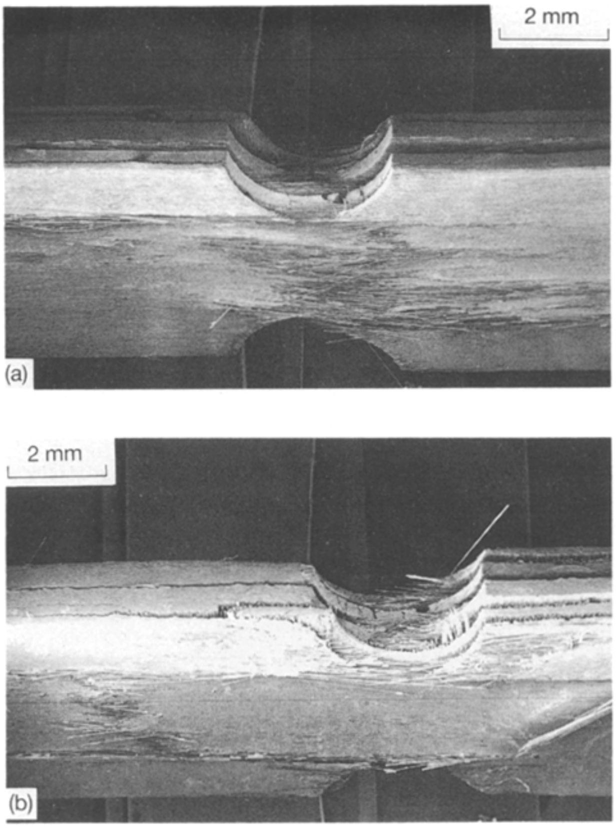

Figure 9 SEM micrographs of the circular DEN specimen, pulled to failure after 400 cycles: (a) surface failure, on the side shown in Fig. 8a and d; (b) surface failure, well away from the notch, on the opposite face.

Similar behaviour has been found in fatigue with unnotched specimens of this material by Zawada *et al.* [28].

2.3.1.2. Rectangular notch. A slightly lower stress level was used in this test, and it was applied for a greater number of cycles. $\Delta\sigma$ was 153 MPa, giving a peak stress around 75% of the static failure stress. After one cycle the damage had just nucleated: there were short splits from the notch root, and delaminations just reached the specimen edge along the notch flanks. Further SEM observations were made after 30, 150 and 800 cycles, and an attempt was made to measure the split length each time. The split tips could be located with reasonable certainty, as the faces had been polished prior to testing. However there was too much scatter in the data, with splits nucleating after widely different numbers of cycles so that the final split lengths at $N = 800$ varied between 0.8 and 6.1 mm. It was also found that delaminations only grew on some 0/90 interfaces. The extensive splits coincided with long delaminations of the same $0°$ ply, so the two types of crack grow together in this material as they do in polymeric composites. There was relatively little damage in the root of the notch after 800 cycles, though some fibres in the central $0°$ ply were bowed, indicating that some irreversible debonding and sliding has taken place (Fig. 10). In time, this behaviour would lead to isolated fibre failures and ply degradation.

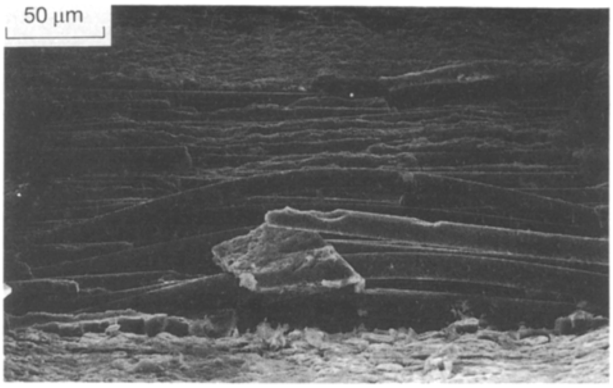

Figure 10 Bowed 0° fibres indicating that some irreversible sliding and damage has occurred.

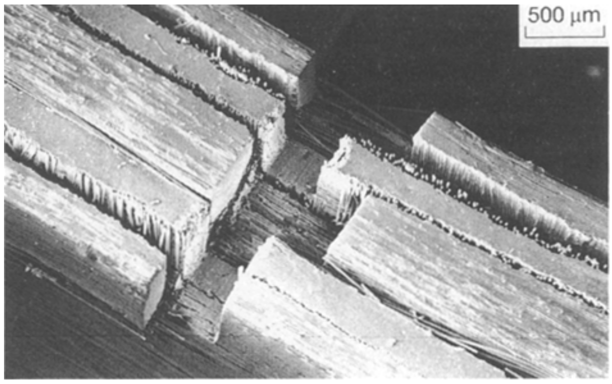

Figure 11 A view of the notch region showing relative sliding of some 0° plies.

The fatigue-damaged specimen was pulled to failure, breaking at a stress of 203 MPa. Again, the failure stress is not significantly different to the static value. The post-fatigue-failed specimen was again more severely damaged than after a static test. As neighbouring plies failed at different locations, mostly away from the notch, the failure caused adjacent plies to slide past one another, leaving a jogged edge to the original notch (Fig. 11).

3. Conclusions

The test series on double-edge-notched tension specimens indicated that the behaviour established for polymeric systems in static and fatigue loading is followed in CAS-glass/SiC laminates up to a point, but significant deviations then occur. The subcritical damage is much more variable in type and location. Splits form from only some of the possible locations, but they then grow easily as the tendency to delaminate is more marked than in CFRP. At failure, there is not a well-characterized damage state as there is in CFRP, making predictive modelling very difficult. The reduction in stress concentration caused by the damage, and the more diffuse locations of fibre failure make the material very notch insensitive.

In fatigue loading, the damage propagates, in principle reducing the notch stress concentration further, but as the fatigue loading degrades the $0°$ ply properties the benefit is lost to some degree. In some cases this can lead to failure, but it was also observed that even when the material has been severely damaged in fatigue its residual strength can still be as high as the initial quasistatic strength.

CAS-glass/SiC composites are more problematic in terms of applying the damage mechanics and modelling used for CFRPs, due to the variability of the damage. This work has highlighted the need for an accurate picture of the subcritical damage before modelling work is undertaken. Dynamic observation has again proved useful in these materials, since at failure the damage propagates rendering post-mortem examination misleading. However, the results are encouraging from the point of view of notch insensitivity, and the retention of strength under moderate fatigue loading.

Acknowledgements
The authors wish to thank Mr Alan Heaver for his practical assistance with all aspects of maintaining and operating the SEM facilities. The financial support of the US Air Force Office of Scientific Research through grant no. AFOSR-87-0307 is gratefully acknowledged.

References

1. H. R. SHERCLIFF, G. VEKINIS and P. W. R. BEAUMONT, *J. Mater. Sci.* **29** (1994) 0000.
2. J. AVESTON, G. A. COOPER and A. KELLY, Proceedings of the National Physical Laboratory Conference on Properties of Fibre Composites Guildford, IPC Science and Technology (1971) p. 15.
3. D. B. MARSHALL, B. N. COX and A. G. EVANS, *Acta Metall.* **33** (1985) 2013.
4. B. BUDIANSKY, J. W. HUTCHINSON and A. G. EVANS, *J. Mech. Phys. Solids* **34** (1986) 164.
5. W. A. CURTIN, *J. Amer. Ceram. Soc.* **74** (1991) 2837.
6. F. W. ZOK and S. M. SPEARING, *Acta Metall. Mater.* **40** (1992) 2033.
7. A. W. PRYCE and P. A. SMITH, *ibid.* **41** (1993) 1269.
8. *Idem., ibid.* in press.
9. D. M. MARSHALL and B. N. COX, *Acta Metall.* **35** (1987) 2607.
10. F. W. ZOK, O. SBAIZERO, C. L. HOM and A. G. EVANS, *J. Amer. Ceram. Soc.* **74** (1990) 187.
11. B. N. COX and D. B. MARSHALL, *Acta Metall. Mater.* **39** (1991) 579.
12. B. N. COX, *ibid.* **39** (1991) 1189.
13. B. N. COX and C. S. LO, *ibid.* **40** (1992) 69.
14. *Idem., ibid.* **40** (1992) 1487.
15. M. T. KORTSCHOT and P. W. R. BEAUMONT, *Compos. Sci. Tech.* **39** (1990) 289.
16. *Idem., ibid.* (1990) 303.
17. M. T. KORTSCHOT, M. F. ASHBY and P. W. R. BEAUMONT, *ibid.* **40** (1991) 147.
18. *Idem., ibid.* **40** (1991) 167.
19. S. M. SPEARING and P. W. R. BEAUMONT, *ibid.* **44** (1992) 159.
20. *Idem., ibid.* **44** (1992) 299.
21. S. M. SPEARING, P. W. R. BEAUMONT and M. F. ASHBY, *ibid.* **44** (1992) 169.
22. S. M. SPEARING, P. W. R. BEAUMONT and P. A. SMITH, *ibid.* **44** (1992) 309.
23. S. M. SPEARING, P. W. R. BEAUMONT and M. T. KORTSCHOT, *Composites* **23** (1992) 305.
24. R. A. DIMANT, H. R. SHERCLIFF and P. W. R. BEAUMONT, unpublished work.
25. M. T. KORTSCHOT, PhD thesis, Cambridge University, Cambridge (1988).
26. F. E. HEREDIA, S. M. SPEARING, A. G. EVANS, P. MOSHER and W. A. CURTIN, *J. Amer. Ceram. Soc.* **75** (1992) 3017.
27. F. E. HEREDIA, S. M. SPEARING, T. J. MACKIN, M. Y. HE, A. G. EVANS, P. MOSHER and P. BRONDSTED, *ibid.* in press.
28. L. P. ZAWADA, L. M. BUTKUS and G. A. HARTMANN, *J. Amer. Ceram. Soc.* **74** (1991) 2851.
29. A. W. PRYCE and P. A. SMITH, *J. Mater. Sci.* **27** (1992) 2695.
30. D. S. BEYERLE, S. M. SPEARING and A. G. EVANS, *J. Amer. Ceram. Soc.* **75** (1992) 3321.

Received 22 October 1993
and accepted 6 January 1994